Cement and Concrete Research 42 (2012) 919–927

Contents lists available at SciVerse ScienceDirect

Cement and Concrete Research

journal homepage: http://ees.elsevier.com/CEMCON/default.asp

Spatially resolved quantitative in-situ phase analysis of a self-leveling compound

Severin Seifert *, Juergen Neubauer, Friedlinde Goetz-Neunhoeffer

Mineralogy, GeoZentrum Nordbayern, Universtity of Erlangen-Nuremberg, Schlossgarten 5a, 91054 Erlangen, Germany

ARTICLE INFO

Article history:
Received 22 October 2011
Accepted 15 March 2012

Keywords:
Hydration (A)
Microstructure (B)
X-ray diffraction (B)
Calcium Aluminate Cement (D)
Mortar (E)

ABSTRACT

The development of the crystalline microstructure of a hydrating self-leveling compound (SLC) was analyzed using a two-dimensional XRD (GADDS). The application of non-destructive micro-diffraction with the GADDS, combined with a custom-made sample holder, made it possible to carry out position-sensitive in-situ measurements of a Calcium–Aluminate–Cement-(CAC)-dominated SLC. Different substrates were used in the measurement procedures so as to acquire data regarding the influence of the properties of the ground surface on the process of hydration. The results show that the crystalline microstructure is strongly affected by the availability of free water. The strongly vertically-fluctuating water-content of the hydrating mortar, which is mainly influenced by outside conditions, has a very significant effect upon the resulting ettringite content. This fact is also reflected in the resulting microstructure of the cured SLC.

1. Introduction

In recent years the application of self-leveling compounds (SLCs) has significantly increased. SLCs are highly developed, polymer-modified dry mortar systems which are mostly used for renovation on uneven substrates in old buildings but also for the construction of new buildings to create a flat and smooth ground surface for final flooring (parquet, carpet, linoleum, tiles, etc.). These dry mortars are ready-to-use mortars, which have only to be mixed with a defined amount of water before they can be applied on site. Depending on the quality of the SLC, its application is carried out in thin layers between 1 and 20 mm thick on different types of substrates (concrete, screed, wood). Furthermore, the demands placed on such a dry mortar system are extremely high, both as regard its workability and its final properties. The properties which such a system needs to possess are, listed in order of importance: self-leveling, low viscosity, fast setting, rapid hardening, rapid strength-gain, rapid drying, dimensional stability, durability, surface strength, and a strong adhesion to the substrate [1]. So as to meet these requirements, SLCs often contain more than ten different inorganic and organic components. These components can be different mineral binders, but most of the SLCs are based on a cement-containing formulation. Generally, this is a fast-setting cement system consisting of a ternary mixture of Ordinary Portland Cement (OPC), Calcium Aluminate Cement (CAC), and calcium sulfate (most commonly bassanite $CaSO_4 \cdot 0.5H_2O$). Additionally, mineral fillers such as limestone flour and quartz sand, as well as different organic and inorganic additives, are added to the dry mix to provide the desired properties. The hydration of the ternary binder system leads to the formation of ettringite ($Ca_6[Al(OH)_6]_2(SO_4)_3 \cdot 26H_2O$) as a major crystalline hydrate phase. It is therefore ettringite which is, along with the organic binders, mainly responsible for the physical properties of the hardened mortar. The hydration of the SLC, and therefore the formation of ettringite, is heavily dependent on the availability of mix water. The application of the SLC in thin layers ($\geq$1 mm) across an area of several square meters results in a very high ratio of surface-to-mortar volume. This may in turn give rise to a rapid desiccation of the mortar due to the evaporation of the mix water at the top surface [2] but also due to the possible absorption of the water by the substrate. Desiccation and loss of water will result in a decrease of hydrate phases, mainly of ettringite content. Consequently, the early strength of the SLC, and also the adhesion of the SLC to the substrate, will be reduced.

There has been very little research published so far about the functionality of SLC or about its hydration process. It is really only a handful of studies that have explored the hydration of different SLCs as well as the influence of the different organic and inorganic components of these SLCs on the hydration process. De Gasparo [3] investigated the distribution and the influence of the organic additives in SLCs and showed that, due to the evaporation of the water, some additives will be enriched in the uppermost millimeter of the mortar layer. Kighelman [4] focused on the hydration process of two ternary binder systems, considering the impact on said process of different additives. This latter study was also able to prove what a strong influence was exerted by a lack of water at the upper layer of the SLCs. This early desiccation of the applied SLC led, it was shown, to a decrease in the degree of hydration in the exposed surface layer.

In the present study, we determined the development of the crystalline phases during hydration with a good vertical resolution in dependence on the underlying substrate. Therefore we used a General Area Detection Diffraction System (GADDS), combined with an in-situ X-ray diffraction technique, to investigate the ongoing hydration process in position-sensitive mode in three different

* Corresponding author. Tel.: +49 9131 8523986.

0008-8846/$ – see front matter © 2012 Elsevier Ltd. All rights reserved.
doi:10.1016/j.cemconres.2012.03.012

areas: namely, near the bottom, in the center, and near the top of the mortar. The benefit of using a 2-D approach as opposed to a conventional XRD system consists in the fact of its offering the possibility of investigating the hydration process under conditions which approximate as closely as possible to its real technical conditions. In an earlier study [5] we presented the results of a qualitative approach. In continuation of this research, we have developed a method for quantifying the increase and the decrease of the crystalline phases during hydration on both a non-water-absorbent and a water-absorbent substrate.

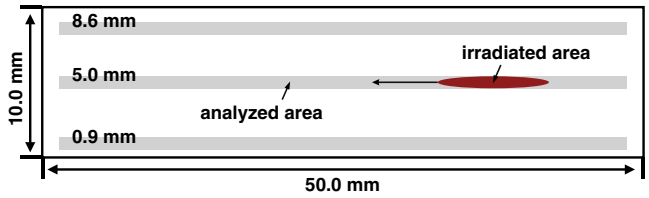

Fig. 1. Sketch of the three measured layers of the 10-mm-thick SLC. The red oval shows the spot of the X-ray beam. By moving the sample under the X-ray beam, a large area is irradiated by the experiment. The gray bars represent the surface areas analyzed.

2. Materials and methods

2.1. Materials and sample preparation

Used in the study was a conventional CAC-based SLC (Table 1). The mortar contained inorganic binders: namely, 50 wt.-% CAC, 30 wt.-% OPC, and 20 wt.-% hemihydrates (α-bassanite) respectively.

For each measurement, 18 g of the dry mortar was mixed with a pre-defined amount of water (w/s = 0.22) for 60 s, using a drilling machine with stirrer. The fresh slurry was then immediately poured into a specially designed and constructed in situ sample holder with an inspection window made of Kapton film which provided a view of a cross section ($50 \times 10\ mm^2$) of the SLC [5]. Due to the defined amount of mortar used, the resulting thickness of the SLC for every measurement was limited to 10 mm. The sample holder was equipped with an exchangeable base, so as to make it possible to simulate either a substrate consisting of a non-absorbent (PVC) material or one consisting of an absorbent material (unglazed ceramic tile; BIII according to standard EN 14411 with 15 wt.-% water-absorption).

2.2. General Area Detection Diffraction System (GADDS)

All measurements were carried out by means of a General Area Detection Diffraction System (GADDS) manufactured by Bruker AXS. This system allows investigation of the SLC in position-sensitive mode [6,7]. The GADDS is equipped with cross-coupled Goebel mirrors at primary X-ray optics side with a pinhole collimator [8]. This optics allows the detection of small areas of the sample, the degree of smallness depending upon the diameter of the collimator used. The two-dimensional HI-STAR detector covers both a wide range of 2-theta, which allows a reduction in the measurement time, and the chi angle, which also serves to promote a rapid process of detection. An advantage of the GADDS technique is that the entire 2-theta range is measured with the same intensity. The lower end of the 2-theta range is not, here, attenuated by primary or secondary apertures. So as to analyze the vertical phase distribution of the hydrating mortar, the SLC was investigated in horizontal slices (Fig. 1). This made it possible to analyze the SLC over a total width of 45 mm. Each layer was measured three times, using three independent preparations, and over a hydration period of 10 h.

By way of an improvement upon previous qualitative measurement data [5], only a single layer was measured within any single preparation. Thus, the measurement time for each single scan was 15 min, while maintaining the time resolution of 40 scans. All in-situ measurements for each layer were repeated three times with the same instrumental parameters. The instrumental parameters used for the investigations (see Table 2) were chosen so as to achieve that specific resolution of the single scans which allows optimized Rietveld refinements for GADDS data. The combination of the collimator pinhole of 300 μm and the constant angle of incidence of the X-ray beam of 9° resulted in a constant elliptical irradiated area (Fig. 1) with a diameter of 1.92 mm to 0.3 mm over the entire measurement range. As a result there was no possibility of a partial overlap of the layers in the X-ray beam at any 2-theta range.

2.3. Rietveld refinement

The resulting diffraction pattern (frame) of each single scan was integrated over 20°chi so as to generate conventional X-ray patterns (intensity versus 2 theta) for the Rietveld refinement. For this reason, there was selected a step size of 0.02°. The refinements were carried out using the software TOPAS 3.0 (Bruker AXS) with fundamental parameter approach. For the determination of the instrumental parameters, as well as the emission profile of the GADDS, a NIST LaB_6 powder was recorded with equivalent parameters. Due to the large number of crystalline phases in the SLC (18 phases in the SLC dry mix and 2 arising hydrate phases), all structural parameters, as well as the crystallite size and the microstrain, were refined using measurements of the individual raw SLC components (OPC, CAC, hemihydrates, limestone flour, milled quartz sand). For the refinement of the phases there were used both unmodified structural parameters (ICSD numbers: 79674, 87088, 174, 79529, 64759, 963, 1841, 100220, 16382, 9197) and structural parameters modified by Goetz-Neunhoeffer [9] (ICSD numbers: 260, 2593, 2842, 27427, 203100, 71916, 30860) (Table 3).

Additionally, for the final refinement of the in-situ measurements the unmodified structure parameters of ettringite (ICSD 155395) [29] and of gypsum (ICSD 92567) (Table 3) were used. The characteristic background caused by the Kapton film was fitted with a background model using pseudo-Voigt functions [30].

For the refinement, three chronological consecutive diffraction patterns ($t_n - 0.25$ h, t_n, and $t_n + 0.25$ h) out of the 40 measurements

Table 1
Composition of the CAC-based self-leveling compound.

Composition	Component	wt.-%
Ternary binder system	Calcium Aluminate Cement (CAC) Ordinary Portland Cement (OPC) α-Bassanite	35.0
Mineral fillers	Limestone flour Chalkstone Quartz sand	61.8
Organic and inorganic additive[a]		3.2

[a] The percentage of the additives results from the known percentages of the other components.

Table 2
X-ray parameters for the quantitative GADDS measurements.

Parameter	Value
X-ray source	Cu Kα
Voltage/current	40 kV/40 mA
Collimator pinhole	300 μm
Measurement angle (2θ)	10° 2θ to 44° 2θ
Measurement angle (chi)	60° (−30° to +30°)
Angle of incidence of X-ray beam (omega)	9°
Spot size of X-ray beam	1.92 × 0.3 mm
Measurement time single scan	15 min
Total measurement time	10 h

Table 3
Overview of the ICSD numbers used for the Rietveld refinement.

Phase	Formula	ICSD	Reference
Calcite	$CaCO_3$	79674	[10]
Dolomite	$CaMg[CO_3]$	87088	[11]
Quartz	SiO_2	174	[12]
Bassanite	$CaSO_4 \cdot 0.5H_2O$	79529	[13]
CA[a]	$CaAl_2O_4$	260	[14]
$C_{12}A_7$[a]	$Ca_{12}Al_{14}O_{33}$	2593	[15]
Ferrat (CAZ)[a]	$Ca_2Fe_{1.43}Al_{0.57}O_5$	2842	[16]
Gehlenite[a]	$Ca_2(Al,Fe)_2SiO_7$	27427	[17]
C_3FT[a]	$Ca_3TiFe_2O_8$	203100	[18]
Perovskite[a]	$CaTiO_3$	71916	[19]
Magnetite[a]	Fe_3O_4	30860	[20]
Alite	Ca_3SiO_5	64759	[21]
β-Belite	Ca_2SiO_4	963	[22]
α′-C_2S	Ca_2SiO_4	–	[23]
C_3A (cub.)	Ca_3AlO_5	1841	[24]
C_3A (orh.)	Ca_3AlO_5	100220	[25]
Anhydrite II	$CaSO_4$	16382	[26]
Ferrat (PZ)	Ca_2FeAlO_5	9197	[27]
Hydrates			
Gypsum	$CaSO_4 \cdot 2H_2O$	92567	[28]
Ettringite	$Ca_6Al_2(SO_4)_3(OH)_{12} \cdot 26H_2O$	155395	[29]

[a] For these phases the modified structures developed by Goetz-Neunhoeffer [9] were used.

were coupled with one another. Thus, the quantity of one refinement is an average value of three chronological consecutive measurements. The first pattern (t = 0.25) and the last pattern (t = 10.0 h) of one in-situ measurement were used twice, for the first and the last refinement respectively. This made it possible to enhance the quantification at the beginning as well as at the end of the measured period. With the exception of the lattice parameter and the crystallite size of ettringite, as well as the preferred orientation of anhydrite, all predetermined structural parameters of the raw SLC components, as well as of any hydrate phases, which were used in addition to these were kept constrained during the refinement. The displacement and the background were individually refined for each pattern. In the first run, the scale factors of all phases were refined. At the same time, the predetermined ratio of certain phases (C_3A cub./C_3A orh., calcite/dolomite, perovskite/magnetite, and C_3FT, C_2S/α′-C_2S) were fixed by constraining the scale factors. The scale factors of inert phases were fixed after the first refinement run. Scale factors of phases, which tend to dissolve or to be precipitated during the hydration process (bassanite, CA, C_3A, anhydrite, ettringite, and gypsum), were refined.

The Rietveld refinement for one layer was repeated twice using measurements from different preparations. This means that the final values represent an average of three different Rietveld refinements.

It is only the quantities of crystalline phases that can be determined by means of Rietveld refinement. The X-ray amorphous phases (e.g. non-bound water, amorphous hydrate phases, and unknown phases) will not be included in such a determination. For this reason, the quantities resulting from the refinement are not absolute quantities. The Rietveld result, then, had to be corrected in consideration of the water contained in the test samples [9] as well as of the amorphous phases and of any definitely known additive content (3.2 wt.-%). At the same time, the corrected result was normalized to the known and constant quartz content of 30 wt.-% [30].

Additionally, the amorphous phase content was estimated using an external standard. The external standard (zirconium silicate powder) was measured using the same parameters as were used for the in-situ measurements of the SLC. Finally, the resulting diffraction pattern of the zirconium silicate was added to the last in-situ pattern of the SLC and subsequently analyzed by Rietveld refinement. The different mass attenuation coefficients of the hardened SLC and the zirconium silicate powder were also taken into account [34].

3. Results

The results for the quantitative phase development of each layer were averaged out from 3 independent preparations. Therefore, the values represent the mean of 3 different measurements.

Generally, the hydration of the ternary binder system is characterized by the formation of ettringite due to the dissolution of CA (from CAC) or C_3A (from OPC) and bassanite. The alite phase C_3S (from OPC) is not involved during the first 10 h of hydration. Consequently, the content of C_3S remains unchanged over the whole hydration time of 10 h (Figs. 3 and 4). Calcite too displays no changes in content during the period investigated.

3.1. Phase development of SLC on non-absorbent substrate

The phase development of the SLC prepared on the non-absorbent substrate shows simultaneous phase development in all three layers. Only in the top layer is the complete hydration process delayed for about 0.5 h. Within the first hour after the addition of the mix water no ettringite can be detected in the bottom and the center layer. About 18 wt.-% of ettringite is formed, however, between 1 h and 3 h. After 3 h, the rate of increase in ettringite formation slows down and reaches a maximum content of 20 wt.-% after 5 h (Fig. 2). This maximum content fits very well with the actual content, which can be calculated from the initial sulfate content (19.9 wt.-% ettringite).

In the top layer, the crystallization of ettringite begins with a delay of about 0.5 h. Furthermore, the maximum ettringite content of 19 wt.-% in the upper layer is slightly lower than in the other two layers (Figs. 2 and 3). The error bars in Fig. 2 show the variations of the phase content of ettringite and CA between the different preparations. The maximum variation of ettringite content of 2.5 wt.-% between 1 h and 3 h results from the rapid kinetic of the ettringite formation within this period. The dissolution of CA and bassanite occurs simultaneously with the formation of ettringite. At the beginning of hydration, the CA and bassanite content remain unchanged. However, 1 h after contact with water the contents of the two phases considerably decrease. Comparably to the formation of ettringite, the dissolution of CA and bassanite in the top layer displays a delay of 0.5 h. In each layer, bassanite dissolves very rapidly. After 2.5 h to 3 h the bassanite has been entirely dissolved in the bottom and center layers, and after 4 h also in the top layer (Fig. 3). Correspondingly to the formation of ettringite, the dissolution of CA is rapid between 1 h and 3 h after addition of water. Subsequently, the decrease in the CA content slows down, and after 6 h CA has dissolved completely (Fig. 2). The highest variation of the determined CA content between the different preparations is 1.3 wt.-%. This is also to be attributed to a very rapid dissolution occurring between 1 h and 3 h.

Due to the very low phase contents of anhydrite as well as of C_3A, the quantification of these phases is difficult. The maximal phase content of anhydrite is 0.9 wt.-%. Nevertheless, a slow decrease in the content of anhydrite is perceptible. After 4 h, the content of anhydrite is below the limit of determination of 0.4 wt.-% (Fig. 3). For this reason, an exact statement about the complete dissolution of anhydrite is not possible. The initial content of C_3A, known from the analysis of the pure OPC and calculated to the SLC-paste, is 0.4 wt.-%. The determination limit for C_3A is 0.4 wt.-%. Therefore no quantitative analysis of C_3A content was possible. Nevertheless, up to the end of the measurement time of 10 h minor contents of C_3A are still detectable (Fig. 3).

In addition to the main hydrate phase, namely ettringite, some gypsum is also simultaneously formed, with a maximum content of 1.1 wt.-%. After 2 h, however, the gypsum begins to dissolve, and

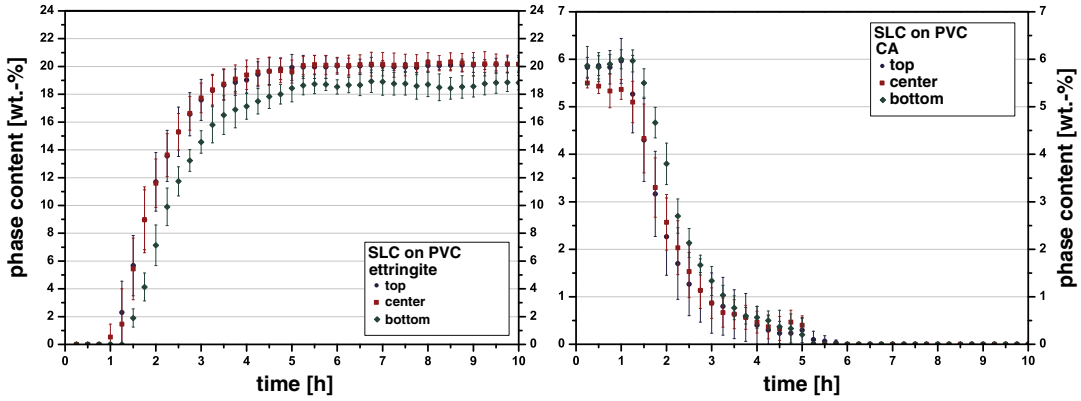

Fig. 2. Phase development of ettringite and CA during the hydration of the SLC on non-absorbent substrate (PVC) according to the measured layers. The curves show an average of three Rietveld refinements.

this coincides with the consumption of the bassanite. Finally, in the bottom and center layer the gypsum has completely dissolved after 3.5 h, and after 4 h also in the top layer (Fig. 3).

The changes in the phase contents in the three layers prove that the process of phase development in the whole SLC is nearly homogeneous in cases where it is applied onto a non-absorbent substrate. The dissolution of CA and bassanite, as well as the formation of ettringite, is comparable between bottom, center and top. Only in the top layer is the phase development delayed for about 0.5 h.

3.2. Phase development of SLC on absorbent substrate

The absorbent substrate strongly affects the hydration of the SLC. The effects can clearly be seen by comparing the various phase developments in the three different layers (Fig. 4).

The formation of ettringite begins after 1 h in the bottom and center layer. The increase in ettringite content in the top layer is delayed for 15 min. In the bottom and center layers, ettringite content increases very rapidly between 1 h and 2 h after addition of water. The increase in the ettringite content slows down until a maximum content of 15 wt.-% is reached after 3.5 h in the center layer and after 4.5 h in the bottom layer. In the top layer, the maximum ettringite content of 8 wt.-% is reached after 3 h (Fig. 5).

The dissolution of the two phases CA and bassanite differs from layer to layer. On the bottom layer, the dissolution of bassanite begins directly after 0.25 h. The bassanite content decreases within the first 2 h very rapidly, and 3.5 h after first contact with water the bassanite has been entirely dissolved. The CA content likewise decreases continuously right from the moment of hydration and stops between 3 h and 3.5 h. Thus, a low CA content of 1 wt.-% is detectable right up to the end of the measurement period (Fig. 5). In the center layer, the bassanite begins to dissolve from the moment of hydration onward and after 3 h the content remains constant at 0.5 wt.-% (Fig. 4). The phase content of CA remains unchanged in the center layer up to the 1 h point. Beyond this point, CA decreases rapidly, down to a constant content of 1.5 wt.-%. This means that the CA will not completely dissolve on the center layer even after 10 h (Figs. 4 and 5). On the top layer, the phase development of bassanite and CA displays a mutually comparable pattern. Only in the first hour is there a difference between the two. While the content of bassanite remains constant, the dissolution of CA begins directly with the commencement of the measurement. After 1 h, the bassanite content also decreases. But after 2 h to 2.5 h the dissolution of these phases ceases. Right up to the end of the measurement at the 10 h point, both phases remain constant, at a content-level of 2.8 wt.-% (Fig. 4).

Quantification of anhydrite, C_3A, and gypsum is, once again, difficult due to the low quantities of these substances present. This difficulty of quantification tends to lead to increasing relative errors. The development of anhydrite is very comparable at the bottom and the center. After 2 h, the phase content decreases, achieving a stable minimum of 0.5 wt.-% after 3 h (Fig. 4). Up to the end of the measurement period, anhydrite is detectable in these two layers. On the top layer, the content of anhydrite remains unchanged over the whole period of 10 h. The C_3A on the top layer displays a similar behavior. On the bottom and the center layer the C_3A dissolves after 2 h and the content decreases below the limit of determination. No dissolution of C_3A on the top layer is detectable. From the initial point of hydration right up to the end of the measurement period the content of C_3A remains constant at 0.7 wt.-% (Fig. 4).

Again, in each layer some gypsum is formed. The crystallization of gypsum begins after 0.5 h and reaches a maximum of 0.5 wt.-% after 1.5 h. On the bottom and center layer the gypsum begins to dissolve after 1.5 h and has entirely dissolved after 3 h. But on the top layer 0.5 wt.-% gypsum remains up to the end of the measurement period (Fig. 4).

The evaluation of the results of the top layer shows a relatively high standard deviation between the individual preparations. The direct comparison of the phase developments within the three layers shows the influence of the absorbent substrate on the hydration of the SLC. First of all, the formation of ettringite, as well as the dissolution of bassanite and CA, is different in each of the measured layers. The amount of ettringite formed tends to increase from the surface as one moves down toward the bottom. The dissolution of anhydrite and C_3A also tends to increase from the surface as one moves down toward the bottom of the SLC.

4. Discussion

The hydration of the CAC-based SLC is characterized by the formation predominantly of the hydrate phase ettringite and by the simultaneous dissolution of CA and bassanite. Initially, after mixing of the SLC dry mix with water, no changes in the phase composition are observable. It is not until at least 1 h has elapsed that the formation of ettringite begins. At the same time the phase contents of CA and bassanite are significantly reduced. Up to this point, the initial contents of bassanite (5.2 ± 0.1 wt.-%) and CA (5.4 ± 0.1 wt.-%) remain constant. Together with the formation of ettringite, we also observe the precipitation of a certain amount of gypsum. This gypsum is a result of the rapid dissolution of bassanite, a phenomenon which has already been described in earlier investigations of ternary binder systems [31,32]. Kighelman [4] too has described areas with accumulations of gypsum in hydrated CAC-based SLC by microstructural investigation. However Kighelman [4] could not confirm the gypsum by X-ray measurements.

Shortly after bassanite depletion the gypsum as well begins to dissolve, thus advancing the further crystallization of ettringite. The dissolution of anhydrite and C_3A begins at the same time and leads to the

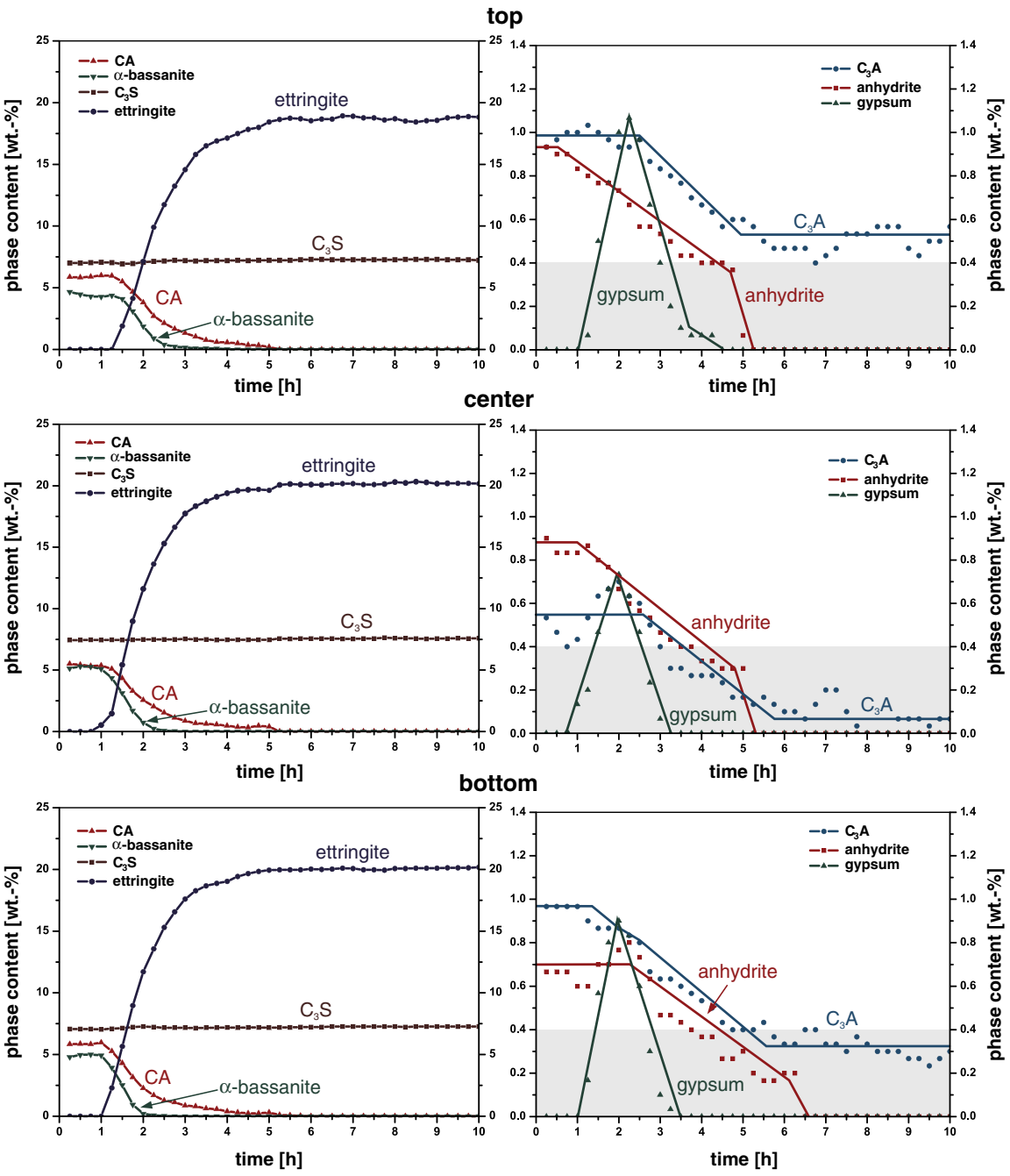

Fig. 3. Phase development of the relevant phases within the SLC during hydration on non-absorbent substrate for the measured layers. Each curve represents the mean values of three independent preparations.

formation of ettringite. Unfortunately, a precise quantification of C_3A is not possible due to the very low content of it present. Bassanite and gypsum have entirely dissolved after 3 h, whereupon the rate of ettringite crystallization is reduced. The process of hydration is then accompanied by a slow dissolution of CA and anhydrite, as well as by a correspondingly slow formation of ettringite. The retarded hydration process is due to the consumption of the available water by this formation of ettringite. Once the CA and anhydrite have been completely consumed after 5 h, the crystallization of ettringite also ceases, and ettringite reaches a maximal content of 20.1 ± 0.1 wt.-%. Subsequently, no further change in phase composition is observable within the 10 h period.

According to the global hydration reaction of a ternary binder system (Eq. (1)), an additional formation of amorphous aluminum hydroxide should occur, due to the absence of an additional calcium source.

$$3CA + 3C\overline{S} + 38H \rightarrow C_3A \cdot 3C\overline{S} \cdot 32H(\text{ettringite}) + 2AH_3 \quad (1)$$

When using the Rietveld refinement system, indeed, it is not possible to determine the quantities of an unknown X-ray amorphous phase without an internal or external standard. For this reason, the final amorphous phase content within the hardened SLC was estimated using an external standard. As a result of this, an amorphous phase content of 8.7 ± 0.5 wt.-% could be determined. Where the known

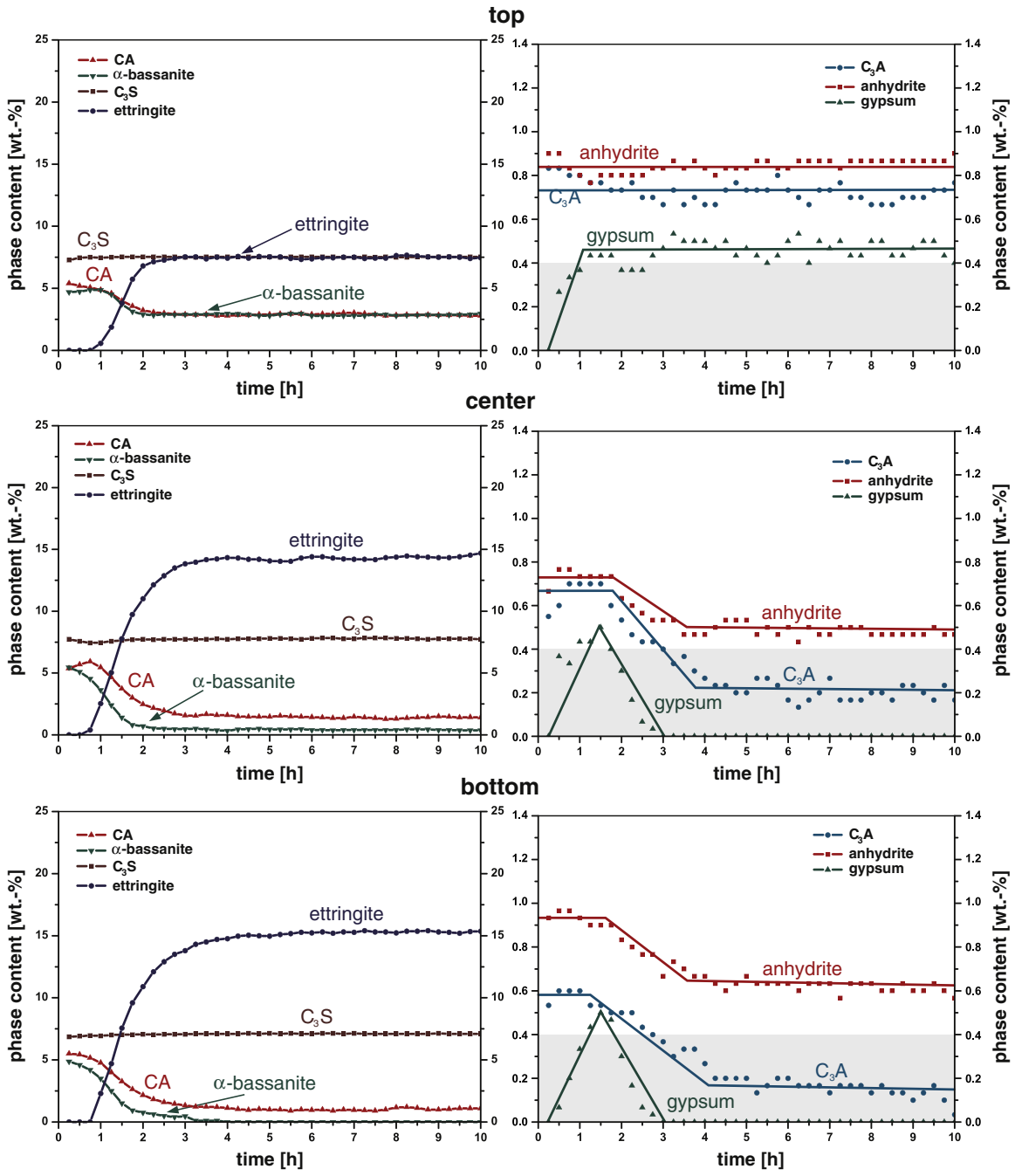

Fig. 4. Phase development of the relevant phases within the SLC during hydration on non-absorbent substrate for the measured layers. Each curve represents the mean values of three independent preparations.

additive content and the established free pore water within the SLC is subtracted there remains an amorphous content of 1.5 wt.-%. This may indicate an additional formation of amorphous aluminum hydroxide (AH_x). Also other studies [4] with other investigation methods prove the simultaneous formation of ettringite and AH_x within a hydrating SLC paste.

The phase C_3S from OPC is not involved during the first 10 h of hydration. This is due to the rapid setting system of the CAC-based SLC. This system is characterized by the formation of ettringite due to the dissolution of CA, C_3A, and bassanite. The slower silicate reaction of C_3S with water cannot proceed because the reaction is running out of water.

The application of the SLC on a non-absorbent substrate leads to very similar hydration in each layer. Only on the top layer close to the surface does the hydration process tend to be delayed for about 0.5 h. Furthermore, the maximal content of ettringite on the top layer after 5 h is reduced as compared to that present on the center and bottom layers. At the same time CA, bassanite, and anhydrite have dissolved completely. Also to be noted is the fact that the C_3A is not fully dissolved in the top layer. The degree of hydration of the SLC near to the surface is lower than in the underlying layers (Fig. 4). This effect is caused by the early desiccation of the SLC paste due to the enhanced evaporation of the water at the surface. This process was also described by the studies of De Gasparo [33] and Kighelman [4]. Thus, a desiccation front arises, which gradually moves from the surface down to the bottom and influences the hydration of the SLC. Due to the high content of water within ettringite – namely, approximately 46 wt.-% – the formation of the latter is inhibited where water is lacking.

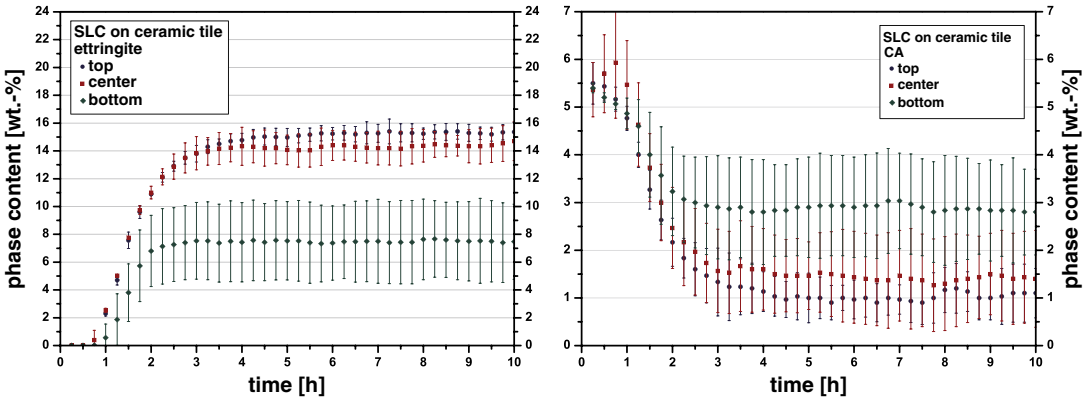

Fig. 5. Phase development of ettringite and CA during the hydration of the SLC on absorbent substrate (ceramic tile) according to the measured layers. The curves show an average of three Rietveld refinements.

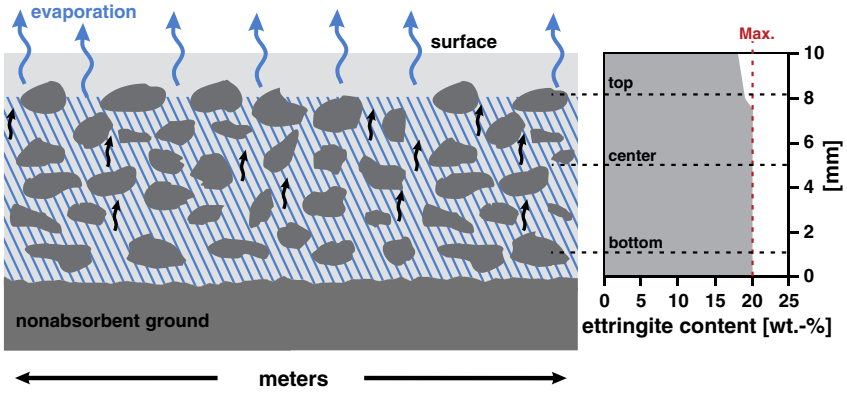

Fig. 6. Sketch of a cross-section of an applied SLC on non-absorbent substrate. The shaded area marks the available water within the SLC. The maximum content of ettringite in the three different layers is shown on the right side. The red dotted line marks the maximum possible content of ettringite calculated from the sulfate content.

A slight lack of water due to evaporation in the upper area of the SLC could be confirmed.

In contrast to non-absorbent substrates, the application on an absorbent substrate strongly influences the hydration of the SLC. These effects are already visible by the macroscopic observation of the cross-section of the hydrated SLC (Fig. 7). The SLC applied on the non-absorbent substrate displays, in terms of color, a homogeneous cross-section. In contrast, the SLC applied on the absorbent substrate clearly displays some differences in color. The cross-section exhibits a gradient in color from the top, which displays a bright matrix, down toward the bottom, which displays a dark matrix. Already this color gradient indicates an inhomogeneous matrix, due to the absorbent ground.

Generally, the hydration of the SLC on the absorbent substrate is comparable to the hydration of the SLC on non-absorbent substrate. The degree of hydration, however, differs significantly. The strong capillary forces of the absorbent substrate reduce the added mix water from the applied SLC. In contrast to what had been supposed, the lower areas are in fact not as strongly influenced as are the upper areas. The availability of free water is reduced due to the absorbent properties of the substrate, with the water soaking through from the upper layer down through the lower layers (Fig. 8). Consequently, the desiccation front again moves from the upper area to the lower areas. Thus, the degree of hydration in the upper area is reduced compared to the lower areas. In spite of the positive properties of the rapid and intensive hydration of the CAC-based SLC, the desiccation

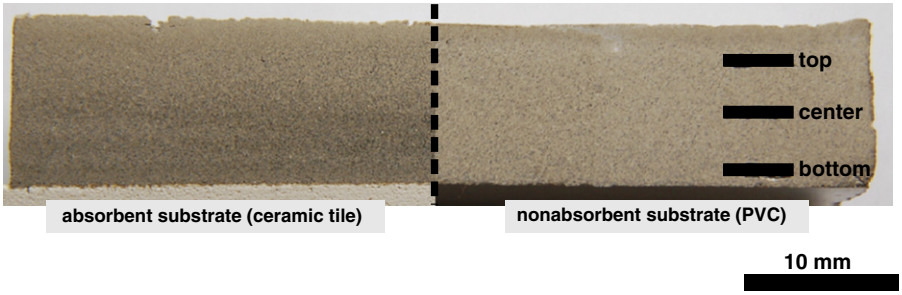

Fig. 7. Comparison of the cross-section of the hydrated SLC on non-absorbent (right) and absorbent (left) substrate. The black lines on the right side mark the three layers investigated (bottom, center, top).

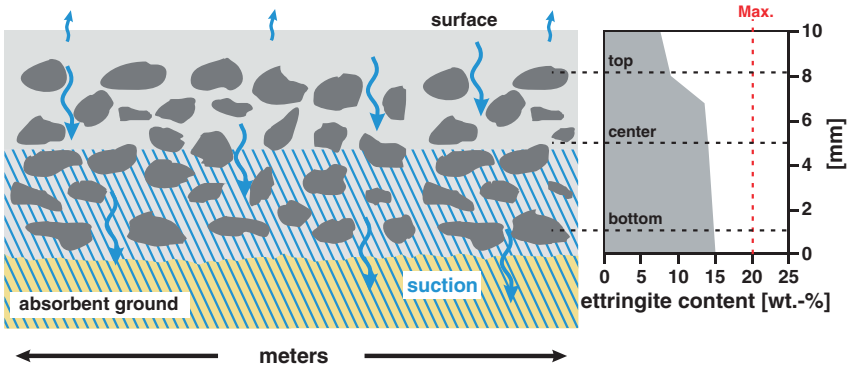

Fig. 8. Sketch of a cross-section of an SLC applied on an absorbent substrate. The shaded area marks the availability of water within the SLC. The maximum content of ettringite in the three different layers is shown on the right side. The red dotted line marks the calculated potential maximum ettringite content.

occurs faster than does the hydration of the SLC. Thus, hydration is restricted by the desiccation front as it proceeds, and is prematurely halted. This effect is reflected in the crystalline phase development of the SLC, which sees a reduction in the maximum ettringite content in the whole SLC. On the top layer, only 8 wt.-% ettringite, which accounts for one third of the possible content, is formed. On the center and bottom layer the ettringite content (15 wt.-%) is lower than observed for the application on a non-absorbent substrate (Fig. 6). Certainly, the effect of the retarder in the SLC is influenced by the migration of the pore water. Thus, the dissolution of CA and bassanite, as well as the formation of ettringite, begins some 0.25 h earlier. Correspondingly to the reduced ettringite content, some unreacted CA and bassanite are also still detectable. In the lower and center layers these contents are very low (0–1 wt.-%) but in the upper layer there are still to be detected 2.8 wt.-% of CA and bassanite, respectively. In addition, the anhydrite is only partially dissolved on the lower layers. On the upper layer the content of anhydrite remains unchanged over the whole 10 h period. Finally, 0.5 wt.-% gypsum remains as a secondary crystalline hydrate phase on the top layer.

The low degree of hydration of an applied SLC can be assumed to be very critical. The reduced formation of ettringite might lead to higher porosity, which could then further reduce the compressive strength of the SLC. Furthermore, the strength development, as well as the bonding, of the SLC is almost exclusively a function of the polymers included [3]. Due to the residues of reactive phases (CA, bassanite, anhydrite, and C_3A) the hydration process could begin again on renewed contact with water, thus resulting in secondary ettringite formation.

5. Conclusion

The present study demonstrates the possibility of investigating the hydration process within a self-leveling compound which is applied as a thin layer on different substrates. Particularly the application of non-destructive microdiffraction with the GADDS, combined with a custom-made sample holder, makes it possible to investigate the hydrating SLC in different horizontal layers. The quantitative analysis of the in-situ measurements using Rietveld refinement of the XRD pattern enables a description of the development of the crystalline phases which are formed and dissolved respectively during hydration.

Regardless of the kind of substrate on which it occurs – non-absorbent or absorbent – the process of hydration of the ternary binder system is basically very similar in all cases. The complete hydration process is mainly based on the formation of the crystalline calcium aluminate hydrate phase ettringite as well as of the X-ray amorphous phase AH_x together with the preliminary dissolution of the cement phases CA, bassanite, anhydrite, and C_3A. In addition to the beginning of ettringite formation at very early stages in the hydration process, a low content of gypsum may also precipitate. However, the initially formed gypsum starts to dissolve shortly after bassanite depletion. The complete hydration process ceases as soon as bassanite, gypsum, anhydrite and CA are consumed. At the same time the ettringite phase content reaches its maximum. It could not be observed that alite (C_3S) from OPC was involved in the hydration process during the first 10 h of hydration. Ettringite is the only hydrate phase which is responsible for the strength during the first 10 h period of hydration.

As a result of the investigations of non-absorbent and absorbent substrates it was shown that the hydration process is strongly influenced and determined by the degree of availability of mix water. The availability of mix water in the different layers of the SLC influences the maximum content of ettringite which can potentially be formed within the hardened SLC. The lack of mix water in the top layer of the SLC does not allow complete hydration of the CA and Ca-sulfates. Therefore the maximum ettringite contents vary within the layers (Fig. 6). At the top of the SLC which was applied on a non-absorbent substrate an evaporation of mix water caused a reduced formation of ettringite as well as a lower degree of hydration. However the hydration in the center and bottom layers was able to proceed unhindered.

The application of the pastes on an absorbent substrate strongly influences the hydration of the SLC. Due to the strong capillary forces of this absorbent substrate, a larger quantity of water is extracted from the SLC, which in turn results in a very rapid desiccation from the top layer down towards the bottom layer. Accordingly, a reduced ettringite content in the whole SLC (Fig. 8) could be determined. Furthermore, the binder phases bassanite, anhydrite and CA do not completely dissolve. The strength development in the top layer is expected to be reduced due to the lower ettringite content. This fact might cause problems when adhesives are used, e.g. in order to fix carpets or other floorings on the surface.

References

[1] H. Motzet, The performance of gypsum based self leveling compounds, in: F. Leopolder (Ed.), Proceedings of the First International Drymix Mortar Conference IDMMC One, Nuremberg, 2007, pp. 26–32.
[2] M. Herwegh, R. Zurbriggen, K. Scrivener, A. De Gasparo, J. Kighelman, A. Jenni, A comparison between Tile Adhesive Mortars (CTA) and Self-leveling Compounds (SLC): what can we learn about the role of polymers in thin-bed mortars? Proceedings of the 16th IBAUSIL (2), Weimar, 2006, pp. 1059–1066.
[3] A. De Gasparo, M. Herwegh, R. Zurbriggen, K. Scrivener, Quantitative distribution of additives in self-leveling flooring compounds (underlayments) as function of application, formulation and climatic conditions, Cem. Concr. Res. 39 (2009) 313–323.
[4] J. Kighelman, Hydration and structure development of ternary binder system as used in self-leveling compounds, Ph.D. Thesis, Écol Polytechnique Fédérale de Lausanne, 2007.

[5] S. Seifert, J. Neubauer, F. Götz-Neunhoeffer, H. Motzet, Characterization of the microstructure of self-leveling compounds (SLC) using 2-dimensional XRD (GADDS), in: Fentiman, et al., (Eds.), Calcium Aluminate Cements: Proceedings of the Centenary Conference 2008, IHS BRE Press, Avignon, 2008, pp. 581–592.
[6] B.B. He, Introduction to two-dimensional X-ray diffraction, Powder Diffr. 18 (2) (2003) 71–85.
[7] S. Seifert, J. Neubauer, F. Goetz-Neunhoeffer, Application of two-dimensional XRD for the characterization of the microstructure of self-leveling compounds, Powder Diffr. 24 (2) (2009) 107–111.
[8] B.B. He, U. Preckwinkel, X-ray optics for two-dimensional diffraction, Adv. X-ray Anal. 45 (2002) 332–337.
[9] F. Goetz-Neunhoeffer, Modelle zur Kinetik der Hydratation von Calciumaluminatzementen mit Calciumsulfat aus kristallchemischer und mineralogischer Sicht, Postdoctoral Thesis, Universtity of Erlangen-Nuremberg, 2006.
[10] R. Wartchow, Datensammlung nach der "Learnt profile"-Methode (LP) für Calcit und Vergleich mit der "Background peak background"-Methode (BPB), Z. Kristallogr. 186 (1989) 300–302.
[11] Y. Suzuki, P.E.D. Morgan, K. Niihara, Use of a high X-ray flux instrument for a mineral: X-ray powder diffraction pattern of $CaMg(CO_3)_2$, Powder Diffr. 13 (4) (1998) 216–221.
[12] Y. Le Page, G. Donnay, Refinement of crystal structure of low-quartz, Acta Crystallogr. B 32 (1976) 2456–2459.
[13] C. Bezou, A. Nonat, J.C. Mutin, A.N. Christensen, M.S. Lehmann, Investigation of crystal structure of γ-$CaSO_4$, $CaSO_4 \cdot 0.5H_2O$, and $CaSO_4 \cdot 0.6H_2O$ by powder diffraction methods, J. Solid State Chem. 117 (1) (1995) 165–176.
[14] W. Hörkner, H. Müller-Buschbaum, Zur Kristallstruktur von $CaAl_2O_4$, J. Inorg. Nucl. Chem. 38 (5) (1976) 983–984.
[15] P.P. Williams, Refinement of the structure of $11CaO \cdot 7Al_2O_3 \cdot CaF_2$, Acta Crystallogr. B 29 (7) (1973) 1550–1551.
[16] A.A. Colville, S. Geller, Crystal structure of $Ca_2Fe_{1.43}Al_{0.57}O_5$ and $Ca_2Fe_{1.28}Al_{0.72}O_5$, Acta Crystallogr. B 28 (11) (1972) 3196–3200.
[17] M. Kimata, N. Ii, The structural property of synthetic gehlenite, $Ca_2Al_2SiO_7$, Neues Jahrbuch Mineral. Abhand. 144 (1982) 254–267.
[18] J. Rodríguez-Carvajal, M. Vallet-Regí, J. Calbet, Perovskite threefold superlattice: a structure determination of $A_3M_3O_8$ phase, Mater. Res. Bull. 24 (4) (1989) 423–430.
[19] R.H. Buttner, E.N. Maslen, Electron difference density and structural parameters in $CaTiO_3$, Acta Crystallogr. B 48 (5) (1992) 644–649.
[20] B.A. Wechsler, D.H. Lindsley, C.T. Perwitt, Crystal structure and cation distribution in Titanomagnetites ($Fe_{3-x}Ti_xO_4$), Am. Mineral. 69 (1984) 754–770.
[21] F. Nishi, Y. Takeuchi, I. Maki, The tricalcium silicate $Ca_3O[SiO_4]$: the monoclinic superstructure, Z. Kristallogr. 172 (1985) 297–314.
[22] K.H. Jost, B. Ziemer, R. Seydel, Redetermination of structure of beta-dicalcium silicate, Acta Crystallogr. B 33 (1977) 1696–1700.
[23] R. Mueller, Stabilisierung verschiedener Dicalciumsilikat-Modifikationen durch Einbau von Phosphat: Synthese, Rietveld-Analyse und Kalorimetrie, Master's Thesis, Universtity of Erlangen-Nuremberg, 2001.
[24] P. Mondal, J.W. Jeffery, The crystal structure of tricalcium aluminate, $Ca_3Al_2O_6$, Acta Crystallogr. B 31 (1975) 689–697.
[25] Y. Takeuchi, F. Nishi, I. Maki, Crystal-chemical characterization of the tricalcium aluminate-sodium oxide ($3CaO \cdot Al_2O_3 - Na_2O$) solid-solution series, Z. Kristallogr. 152 (3–4) (1980) 259–307.
[26] A. Kirfel, G. Will, Charge density in anhydrite, $CaSO_4$, from X-ray and neutron diffraction measurements, Acta Crystallogr. B 36 (1980) 2881–2890.
[27] A.A. Colville, S. Geller, The crystal structure of brownmillerite, Ca_2FeAlO_5, Acta Crystallogr. B 27 (12) (1971) 2311–2315.
[28] P.F. Schofield, C.C. Wilson, K.S. Knight, I.C. Stretton, Temperature-related structural variation of the hydrous components in gypsum, Z. Kristallogr. 215 (12) (2000) 707–710.
[29] F. Goetz-Neunhoeffer, J. Neubauer, Refined ettringite ($Ca_6Al_2(SO_4)_3(OH)_{12} \cdot 26H_2O$) structure for quantitative X-ray diffraction analysis, Powder Diffr. 21 (1) (2006) 4–11.
[30] S. Seifert, Ortsaufgelöste Phasenanalyse an selbstverlaufenden Bodenspachtelmassen, Ph.D. Thesis, Universtity of Erlangen-Nuremberg, 2009.
[31] F. Goetz-Neunhoeffer, R. Zurbriggen, Formation of hydrate spheres in ternary binder systems, ZKG Int. 61 (12) (2008) 68–76.
[32] C. Evju, S. Hansen, Expansive properties of ettringite in a mixture of calcium aluminate cement, Portland cement and beta-calcium sulfate hemihydrate, Cem. Concr. Res. 31 (2) (2001) 257–261.
[33] A. De Gasparo, Fractionation behavior of organic additives and resulting microstructural evolution of mixed-binder based self-leveling flooring compounds, Ph.D Thesis, University of Bern, 2006.
[34] D. Jansen, F. Goetz-Neunhoeffer, Ch. Stabler, J. Neubauer, A remastered external standard method applied to the quantification of early OPC hydration, Cem. Concr. Res. 41 (2011) 602–608.